CROMER, D. T. (1969). J. Chem. Phys. 50, 4857-4859.
CROMER, D. T. & LIBERMAN, D. (1970). J. Chem. Phys. 53, 1891-1898.
DOYLE, P. A. & TURNER, P. S. (1968). Acta Cryst. A24, 390-397.
EPPERSON, J. E. & FÜRNROHR, P. (1983). Acta Cryst. A39, 740-746.
GEHLEN, P. C. & COHEN, J. B. (1965). Phys. Rev. A, 139, 844-855.
GEORGOPOULOS, P. & COHEN, J. B. (1977). J. Phys. 12, C7, 191-196.
GEORGOPOULOS, P. & COHEN, J. B. (1981). Acta Metall. 29, 1535-1551.
GRAGG, J. E. & COHEN, J. B. (1971). Acta Metall. 19, 507-519.
GRÖHLICH, M., HAASEN, P. & FROMMEYER, G. (1982). Scr. Metall. 16, 367-370.
KOSTORZ, G. (1983). In Physical Metallurgy, 3rd ed., edited by R. W. CAHN & P. HAASEN, pp. 793-853. New York: North-Holland.
LEFEBVRE, S., BLEY, F., BESSIÈRE, M., FAYARD, M., ROTH, M. & COHEN, J. B. (1980). Acta Cryst. A36, 1-7.
LEFEBVRE, S., BLEY, F., FAYARD, M. & ROTH, M. (1981). Acta Metall. 29, 749-761.
LE PAGE, Y., GABE, E. J. & CALVERT, L. D. (1979). J. Appl. Cryst. 12, 25-26.

MATSUBARA, E. & COHEN, J. B. (1983). Acta Metall. 31, 2129-2135.
OHSHIMA, K.-I., WATANABE, D. & HARADA, J. (1976). Acta Cryst. A32, 883-892.
POTTEBOHM, H., NEITE, G. & NEMBACH, E. (1983). Mater. Sci. Eng. 60, 189-194.
SCHWARTZ, L. H. & COHEN, J. B. (1977). Diffraction from Materials. New York: Academic Press.
SPARKS, C. J. & BORIE, B. (1965). In Local Atomic Arrangements Studied by X-ray Diffraction, edited by J. B. COHEN & J. E. HILLIARD, pp. 3-50. New York: Gordon & Breach.
WARREN, B. E. (1969). X-ray Diffraction. Reading, MA: Addison-Wesley.
WENDT, H. & HAASEN, P. (1983). Acta Metall. 31, 1649-1659.
WILLIAMS, R. O. (1972). A Computer Program for the Reduction of Diffuse X-ray Data from Solid Solutions. Report ORNL-4828. Oak Ridge National Laboratory, Oak Ridge, Tennessee, USA.
WILLIAMS, R. O. (1976). A Computer Program for the Simulation of Solid Solutions. Report ORNL-5140. Oak Ridge National Laboratory, Oak Ridge, Tennessee, USA.
WU, T. B., MATSUBARA, E. & COHEN, J. B. (1983). J. Appl. Cryst. 16, 407-414.

Difference Fourier Syntheses in Fiber Diffraction

BY KEIICHI NAMBA* AND GERALD STUBBS

Department of Molecular Biology, Vanderbilt University, Nashville, TN 37235, USA

Abstract

Theory applying to difference Fourier syntheses from fiber diffraction data is developed, including the calculation of expected peak heights and noise levels. The signal-to-noise ratio in fiber diffraction difference maps is much lower than in crystallography, because of the multi-dimensional nature of fiber diffraction data, but it is shown by means of examples from tobacco mosaic virus that high-order difference syntheses, for example using coefficients analogous to crystallographic $6F_{obs} - 5F_{calc}$, can clearly reveal differences between an observed structure and a model. 'Omit' maps, calculated from models by omitting a region under particular scrutiny, are of limited use in fiber diffraction, but maps calculated from hybrid coefficients derived from both full and partial models have some applications.

Introduction

Difference syntheses have been widely used in both protein and small-molecule crystallography to deter-

mine structures related to already known structures, and as part of refinement procedures (Blundell & Johnson, 1976; Glusker & Trueblood, 1985). Although they have found some use in fiber diffraction [a number of references are given by Mandelkow, Stubbs & Warren (1981)], this use has until now been limited by the difficulties peculiar to fiber diffraction which arise from the cylindrical averaging of fiber diffraction patterns. Difference Fourier maps calculated from fiber diffraction data by direct analogy with crystallographic difference maps tend to have high noise levels and to be biased toward the known or model structure, as will be shown below. In favorable cases, modification of the model structure has enabled interpretable maps to be calculated (Mandelkow, Stubbs & Warren, 1981), but no systematic procedure has been available to deal with the general case.

In this paper, we develop the theory of fiber diffraction difference Fourier syntheses, and illustrate the method with examples that use simulated data sets, calculated from an atomic model of tobacco mosaic virus (TMV). We also present several alternative, semi-empirical syntheses, that have proven effective in handling real data.

---

* Present address: ERATO, 5-9-5 Tokodai, Toyosato, Tsukuba 300-26, Japan.

Theory

In a fiber diffraction experiment, the diffracted intensity at reciprocal-space radius R on layer line l is

$$I(R, l) = \sum_n G_{n,l}(R) G^*_{n,l}(R) \qquad (1)$$

(Waser, 1955; Franklin & Klug, 1955), where n is the order of the Bessel functions J_n that contribute to the complex Fourier-Bessel structure factor G (Klug, Crick & Wyckoff, 1958). For a helical structure, n is restricted by the selection rule $l = tn + um$, where m is an integer and there are u subunits in t turns of the helix. The number of significant terms contributing to the intensity in (1), denoted here by N, depends on the symmetry and dimensions of the diffracting particle, and on the value of (R, l). For example, for TMV at 2·9 Å resolution, N can be as much as 8. Equation (1) can be compared with the crystallographic equation

$$I(h, k, l) = F_{hkl} F^*_{hkl}.$$

If each G is known, an electron density map may be obtained from the relationships

$$\rho(r, \varphi, z) = (1/c) \sum_{l=-\infty}^{\infty} \sum_{n=-\infty}^{\infty} g_{n,l}(r)$$

$$\times \exp[i(n\varphi - 2\pi l z/c)] \qquad (2)$$

and

$$g_{n,l}(r) = \int_0^{\infty} G_{n,l}(R) J_n(2\pi R r) 2\pi R \, dR \qquad (3)$$

where ρ is electron density; r, φ and z are cylindrical coordinates in real space; and c is the repeat distance in the diffracting structure. The Fourier-Bessel transform represented by (2) and (3) is analogous to the Fourier transform of the F terms in crystallography. The problem of determining the values of the G terms, the phase problem for fiber diffraction, has been addressed in earlier papers (Stubbs & Diamond, 1975; Stubbs & Makowski, 1982; Namba & Stubbs, 1985).

It is useful to define a $2N$-dimensional vector $\mathscr{G}$, whose components are the components of the N significant G terms contributing to a particular intensity $I(R, l)$ in (1). Then (2) and (3) can be written

$$\rho = T_{\text{FB}}(\mathscr{G})$$

where T_{FB} is the Fourier-Bessel transform. The difference in electron density between the unknown structure and a known or model structure (denoted by the subscript 0) is

$$\Delta\rho = T_{\text{FB}}(\mathscr{G}) - T_{\text{FB}}(\mathscr{G}_0) = T_{\text{FB}}(\mathscr{G} - \mathscr{G}_0).$$

This is a multi-dimensional analog of the two-dimensional case found in crystallography, where, if T_F represents a Fourier transform,

$$\Delta\rho = T_{\text{F}}(\mathbf{F} - \mathbf{F}_0).$$

$\Delta\mathbf{F} = \mathbf{F} - \mathbf{F}_0$ is not available experimentally, but if the known and unknown structures are believed to be similar, it is customary to use instead a vector having the phase of $\mathbf{F}_0$ and magnitude $\Delta F = F - F_0$. For small ΔF, this vector approximates to $\mathbf{F}_{\text{IP}}$, the component of $\Delta\mathbf{F}$ in phase with $\mathbf{F}_0$ (Fig. 1).

Peak heights

Difference Fourier syntheses have been shown to contain electron density peaks which, when ΔF is small compared with F (that is, when the unknown part of the structure is small), approach half their true height (Luzzati, 1953). Henderson & Moffat (1971) give a simplified derivation of this height, pointing out that the contribution of $\mathbf{F}_{\text{IP}}$ in the direction of $\Delta\mathbf{F}$ is $\Delta F \cos^2 \theta$, where θ is the angle between $\mathbf{F}_{\text{IP}}$ and $\Delta\mathbf{F}$, and that since $\Delta\mathbf{F}$ is not correlated with $\mathbf{F}_0$, the mean contribution to the electron density is weighted by $\langle \cos^2 \theta \rangle = \frac{1}{2}$. The phase triangle in Fig. 1 can equally well be constructed from $\mathscr{G}_0$, $\mathscr{G}$ and $\Delta\mathscr{G}$, and although it is then embedded in hyperspace, it is still two-dimensional. However, in $2N$-dimensional space, $\langle \cos^2 \theta \rangle = 1/2N$ (see Appendix*), so although the arguments given above still apply, in the absence of noise the peaks in a difference Fourier-Bessel synthesis from fiber diffraction data are expected to have $1/2N$ times their true heights, or $1/N$ times the heights of comparable peaks in a crystallographic difference Fourier map.

Noise levels

In order to determine the mean square error in electron density inherent in the difference Fourier-Bessel method, we will follow the crystallographic approach of Henderson & Moffat (1971) and Blow & Crick (1959), generalized to $2N$ dimensions. This

---

* The Appendix proving this result has been deposited with the British Library Document Supply Centre as Supplementary Publication No. SUP 43621 (3 pp.). Copies may be obtained through The Executive Secretary, International Union of Crystallography, 5 Abbey Square, Chester CH1 2HU, England.
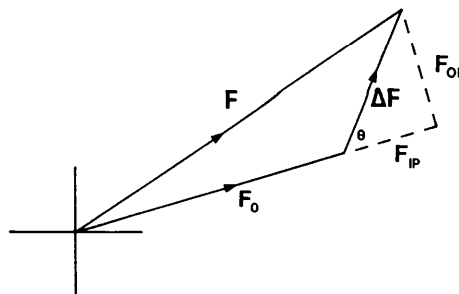

Fig. 1. Structure factors from a known structure, F_0, a similar but otherwise unknown structure, F, and thier difference, ΔF. F_{IP} and F_{OP} are the in-phase and out-of-phase components of ΔF. This phase triangle describes equally well the multi-dimensional vectors $\mathscr{G}_0$, $\mathscr{G}$ and $\Delta\mathscr{G}$.

is possible, as shown below, because of the equality $\langle F^2 \rangle = \langle \mathscr{G}^2 \rangle$. We will consider only those errors inherent in the method, and not errors of intensity measurement or errors in the model structure. Because $\Delta\mathscr{G}$ is not correlated with $\mathscr{G}$, its $2N$ orthogonal components have equal expectation values, as do the two orthogonal components of $\Delta\mathbf{F}$. However, whereas in the two-dimensional case there is only one unknown component $(\mathbf{F}_{OP})$, in $2N$ dimensions $2N-1$ unknown components contribute to the error in the electron density. Thus, as we will show in this section, the mean square error inherent in difference Fourier–Bessel syntheses is $2N-1$ times as great as in difference Fourier syntheses.

The mean square error in a difference electron density map is

$$\langle \Delta\Delta\rho^2 \rangle = (2/V^2) \sum |\Delta\Delta\mathbf{F}|^2$$

where $\Delta\Delta\mathbf{F}$ is the error in the estimate of $\Delta\mathbf{F}$, i.e. $\mathbf{F}_{OP}$. $\mathbf{F}_{IP}$ and $\mathbf{F}_{OP}$ are uncorrelated components of $\Delta\mathbf{F}$, so $\sum F_{OP}^2 = \sum F_{IP}^2$, and for small values of ΔF, $F_{IP} \simeq \Delta F$, so

$$\langle \Delta\Delta\rho^2 \rangle = (2/V^2) \sum \Delta F^2.$$

In fiber diffraction, ΔF is not directly available, and the difference synthesis is based on $\mathscr{G} - \mathscr{G}_0$. Nevertheless, we can estimate $\sum |\Delta\Delta\mathbf{F}|^2$, using the relationship

$$\mathbf{F} = \sum_j \mathbf{G}_j \exp in(\psi + \pi/2)$$

(Klug, Crick & Wyckoff, 1958). ψ is the azimuthal coordinate in reciprocal space. If $\mathbf{G}_j \exp in(\psi + \pi/2) = A_j + iB_j$, then

$$F^2 = \sum_j A_j^2 + \sum_j B_j^2 + \sum_{j,k} (A_j A_k + B_j B_k)$$

and if we sum over all reciprocal space, with the uncorrelated cross terms dropping out,

$$\sum F^2 = \sum \left[\sum_j (A_j^2 + B_j^2) \right] = \sum \mathscr{G}^2. \qquad (4)$$

Now

$$\langle \Delta\Delta\rho^2 \rangle = (2/V^2) \sum |\Delta\Delta\mathscr{G}|^2 = (2/V^2) \sum \mathscr{G}_{OP}^2.$$

$\Delta\mathscr{G}$ has $2N$ components, all having equal expectation values. One of those components is $\mathscr{G}_{IP}$, while the sum of the remaining $2N-1$ components, $\Delta\Delta\mathscr{G}$, is $\mathscr{G}_{OP}$, so $\sum \mathscr{G}_{OP}^2 = (2N-1) \sum \mathscr{G}_{IP}^2 = (2N-1) \sum \Delta\mathscr{G}^2$, where $\Delta\mathscr{G} = \mathscr{G} - \mathscr{G}_0$. Therefore

$$\langle \Delta\Delta\rho^2 \rangle = [2(2N-1)/V^2] \sum \Delta\mathscr{G}^2;$$

so, from (4),

$$\langle \Delta\Delta\rho^2 \rangle = [2(2N-1)/V^2] \sum \Delta F^2.$$

This is the expression for the mean square noise level inherent in the difference Fourier method in fiber diffraction. The noise level is higher than the level in crystallography by a factor of $(2N-1)^{1/2}$.

Application to simulated data

We have applied the theory described above to simulated, error-free data. These data were used in preference to real data in order to examine specifically limitations imposed by the noise inherent in the method. Practical applications using real data are considered below.

A set of intensity data was generated from the atomic coordinates found for TMV (Namba & Stubbs, 1985, 1986). These were treated as 'observed' data. The coordinates were perturbed in various regions using the program *FRODO* (Jones, 1982) in conjunction with an Evans and Sutherland PS300 computer graphics system, in order to generate numerous sets of 'calculated' data. Similar results were obtained from all of these sets. Examples from two are described here: one in which only the side chain of Arg 112 was perturbed, and one in which the entire structure of residues 64–67 was perturbed.

Difference maps

In crystallography, the simplest form of difference map is calculated from coefficients $F - F_0$ and phases taken from $\mathbf{F}_0$. These maps ideally represent $\frac{1}{2}\Delta\rho$, where the true electron density ρ is equal to $\rho_0 + \Delta\rho$, and ρ_0 is the electron density in the model structure. Coefficients F with phases from $\mathbf{F}_0$ lead to electron densities $\rho_0 + \frac{1}{2}\Delta\rho$; thus, the widely used synthesis with coefficients $2F - F_0$ is intended to calculate $\rho_0 + \frac{1}{2}\Delta\rho + \frac{1}{2}\Delta\rho = \rho$. In practice, the unknown part of the structure (which includes errors in the model structure) may not be negligible, and there will be errors in the structure amplitudes, so the coefficient of $\Delta\rho$ may be less than $\frac{1}{2}$ (Luzzati, 1953; Henderson & Moffat, 1971). In order to allow for this effect, higher-order difference Fourier maps with coefficients such as $3F - 2F_0$ have sometimes been calculated (e.g. Deisenhofer & Steigemann, 1975; Artymiuk & Blake, 1981).

From the theory developed above, it is evident that in fiber diffraction simple difference maps will be images of $1/2N$ times the true difference density, where N is some average value of the number of overlapping terms contributing to the diffracted intensities in (1). In practice, these images may be weaker because of errors in the intensities and in the model structure. In order to obtain the best possible representation of ρ, a difference Fourier–Bessel synthesis should be calculated with coefficients $n\mathscr{G} - (n-1)\mathscr{G}_0$, where n is a number that varies across the data set, being twice the number of overlapping terms at each data point. n will generally be significantly larger than is usual in crystallography. In Fig. 2(b) we present such a synthesis for the model perturbation at residues 64–67. It is evident that such syntheses work well, particularly by comparison with the direct

analog of one of the most common syntheses used in crystallography, $2\mathscr{G} - \mathscr{G}_0$ (Fig. 2a).

We have found that with real data these very high-order syntheses can be rather noisy, because of the extreme reinforcement of the high-resolution contributions, including noise, to the image. A simple empirical approach that has worked well in the case of TMV is to use moderate-order values of n, and not to vary them across the data set. This effectively weights down the high-reciprocal-space-radius contribution to the map. Fig. 2(c) is an example of such a synthesis with $n = 6$ for the region of TMV shown in Fig. 2(a). Fig. 3 presents examples of such syntheses for the Arg 112 region, over a range of values for n. It is evident from Figs. 3(d), (e) and (f) that, although it is important to choose a suitable value for n, the exact value is not critical. Even so, it is clear from Figs. 3(a), (b) and (c) that the most common syntheses used in crystallography, with $n = 1, 2$ and 3, are not generally suitable for fiber diffraction. For a system with the symmetry of TMV at 2·9 Å resolution, where $N = 8$, a value for n of about 5 or 6 seems to be very satisfactory.

Omit maps

Although the difference maps described in the previous section should prove satisfactory for most applications, there are circumstances in which it is extremely desirable to minimize any possible bias towards a model structure. In recent years, 'omit maps' have become popular as a means to this end. These maps are calculated from observed structure-factor amplitudes and calculated phases, but in the phase calculation the part of the structure under scrutiny is omitted. In a series of maps, sections of the unit cell can be systematically omitted (Artymiuk & Blake, 1981). Alternatively, parts of the model structure can be omitted; for example, Furey, Robbins, Clancy, Winge, Wang & Stout (1986) omitted three peptide residues at a time. A similar approach was taken in a fiber diffraction study by Mandelkow, Stubbs & Warren (1981), who omitted electron density corresponding to amino acid side chains suspected of changing conformation between two different forms of TMV protein. In some cases they obtained definite results: omitted density returned, or included density disappeared. In other cases, however, the noise level was too high to allow unambiguous interpretations to be made.

The size of the omitted structure has considerable bearing on the interpretability of omit maps. This is particularly so with fiber diffraction data, because the ratio of model observations to diffracted data observations is much higher than in crystallography. For very small omissions, such as a single side chain, we have obtained results similar to those illustrated in Fig. 3, but with larger omissions there is a sig-

nificant loss of interpretability. Omission of ten of the 158 residues of TMV protein led to almost uninterpretable maps; the maps from low-order syntheses such as $2\mathscr{G} - \mathscr{G}_0$ are too weak for more than partial
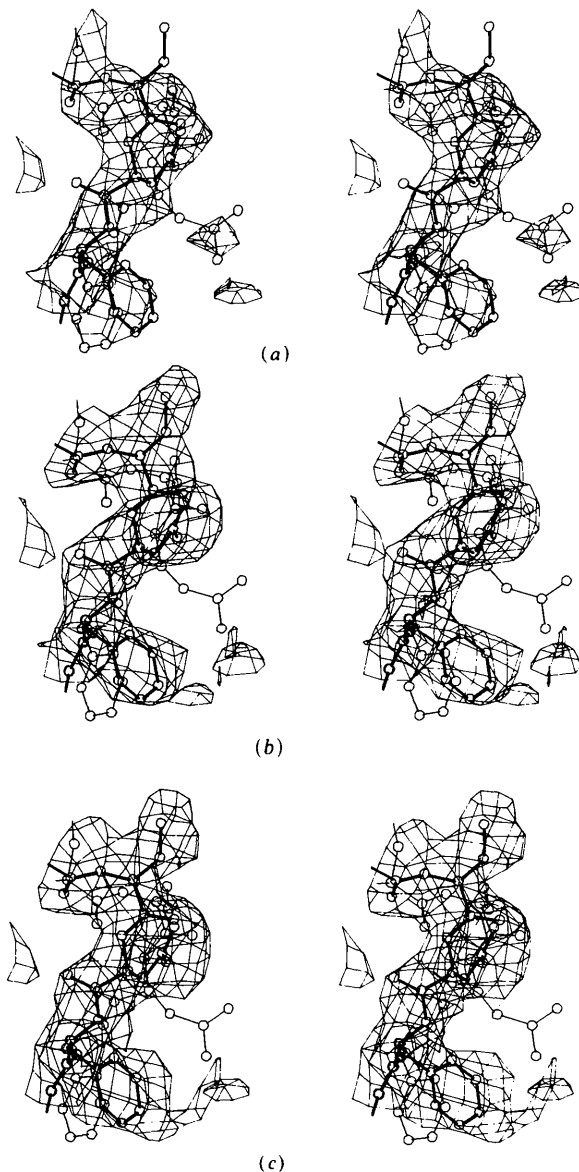

(a)

(b)

(c)

Fig. 2. (a) A difference map at 2·9 Å resolution calculated from simulated TMV data, with residues 64 to 67 perturbed. The coefficients used were $2\mathscr{G} - \mathscr{G}_0$. This is directly analogous to one of the most common crystallographic syntheses, but is clearly not suited to fiber diffraction analysis in this case. (b) A map of the same part of the structure, in which the coefficient used for each data point was $n\mathscr{G} - (n-1)\mathscr{G}_0$, where n is twice the number of overlapping terms contributing to that point. This is the theoretically correct coefficient. The largest value of n used in this case was 16. (c) A map of the same part of the structure, using coefficients $6\mathscr{G} - 5\mathscr{G}_0$. This type of map is a convenient and accurate alternative to (a), and with real data is often less noisy than (a). Heavy lines: the TMV model used as the 'true' structure, to provide amplitudes. Light lines: the perturbed structure, used to provide 'calculated' structure factors.

interpretation (Fig. 4a), while higher-order maps such as $6\mathscr{G} - 5\mathscr{G}_0$ give the impression of a severe loss in resolution (Fig. 4b). It therefore appears that while omit maps can be of value to fiber diffractionists in answering questions about small regions of a molecule, they are not suitable for the systematic examination of complete structures.

Hybrid maps

The data discarded in an omit map may include sources of reliable information. Ideally one should not discard them, but include them at some reduced weight. Alternatively, the Fourier synthesis can include weights based on the agreement between calculated and observed structure factors (Sim, 1959;

Blundell & Johnson, 1976), but such a weighting scheme has not yet been fully devised for fiber diffraction (Namba & Stubbs, 1985).

We have experimented with a variety of different coefficient combinations drawing on data calculated from both complete and partial structures. Useful maps have been obtained using Bessel order terms in (1) separated on the basis of complete structures, but with phases based on partial structures. [Such a distinction is arbitrary, since all the real and imaginary parts of each G in (1) are mutually orthogonal, but it is computationally convenient.] The coefficients used in the Fourier–Bessel synthesis were $\{G'\}$, vectors with phases calculated from the partial structure and amplitudes $G' = 2G'' - G_{omit}$. G_{omit} is calculated from the partial structure and G'' is obtained from
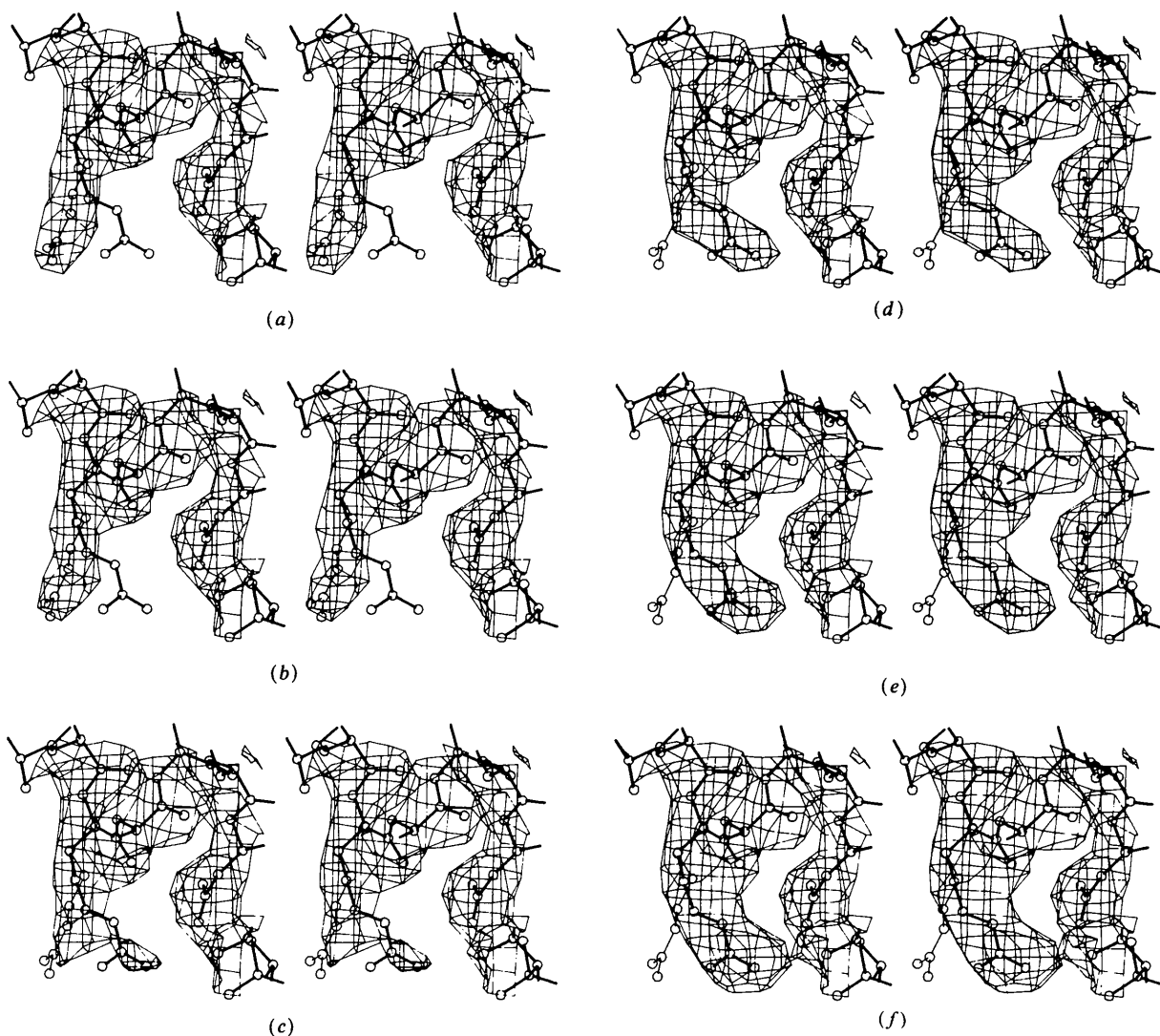

(a)

(b)

(c)

(d)

(e)

(f)

Fig. 3. High-order difference maps calculated from simulated TMV data, with the side chain of Arg 112 perturbed. Coefficients used were: (a) $\mathscr{G}$; (b) $2\mathscr{G} - \mathscr{G}_0$; (c) $3\mathscr{G} - 2\mathscr{G}_0$; (d) $4\mathscr{G} - 3\mathscr{G}_0$; (e) $5\mathscr{G} - 4\mathscr{G}_0$; (f) $6\mathscr{G} - 5\mathscr{G}_0$. The higher-order maps provide an accurate representation of the correct structure. Heavy lines: the TMV model used as the 'true' structure, to provide amplitudes. Light lines: the perturbed structure, used to provide 'calculated' structure factors.

$m\mathcal{G} - (m-1)\mathcal{G}_0$, divided into Bessel order terms in the same ratio as $\mathcal{G}_0$. We describe such a coefficient (*e.g.* for $m = 3$) with the convention

$$\mathcal{G}' = [2(3\mathcal{G} - 2\mathcal{G}_0) - \mathcal{G}_{omit}]\alpha_{omit}.$$

Figs. 4(c) and 5 present maps calculated from these hybrid coefficients. In Fig. 5 a range of values of m

is used. The best results were obtained with m equal to 3; this map is related to the high-order difference map in Fig. 3 with $n = 6$. Calculations such as these can be used for scanning an entire structure relatively quickly, since significant parts of the model structure can be left out of each map; thus some of the advantages of both direct and omit difference syntheses are combined.

Application to real data

Determination of relatively large molecular structures on the basis of fiber diffraction data is becoming
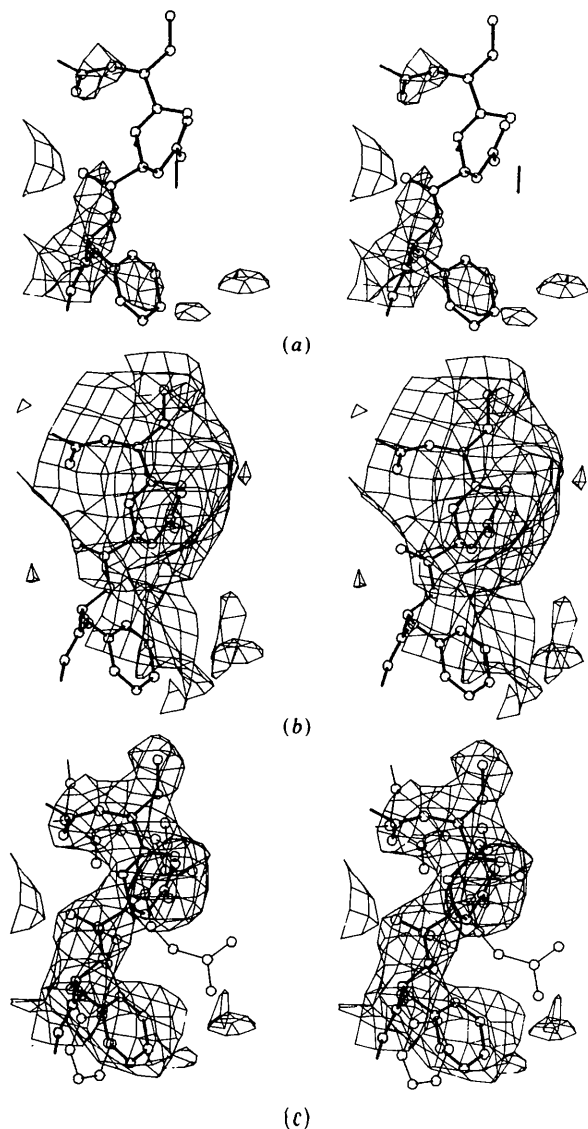

Fig. 4. (a) 'Omit' map calculated from simulated TMV data, with residues 64–67 perturbed. The coefficients used were $2\mathcal{G} - \mathcal{G}_{omit}$, where $\mathcal{G}_{omit}$ was calculated from the TMV structure with residues 61–70 omitted. Most of the omitted structure is not visible in the map. (b) 'Omit' map using the higher-order coefficients $6\mathcal{G} - 5\mathcal{G}_{omit}$. Although the omitted structure is now in density, there is very little detail present. (c) A map using Bessel order separations from the complete perturbed structure, and phases of G terms from the partial structure. Heavy lines: the TMV model used as the 'true' structure. Light lines: the perturbed structure. Coefficients used were (in the convention defined in the text) $[2(3\mathcal{G} - 2\mathcal{G}_0) - \mathcal{G}_{omit}]$. This synthesis combines advantages of both direct and 'omit' difference maps.
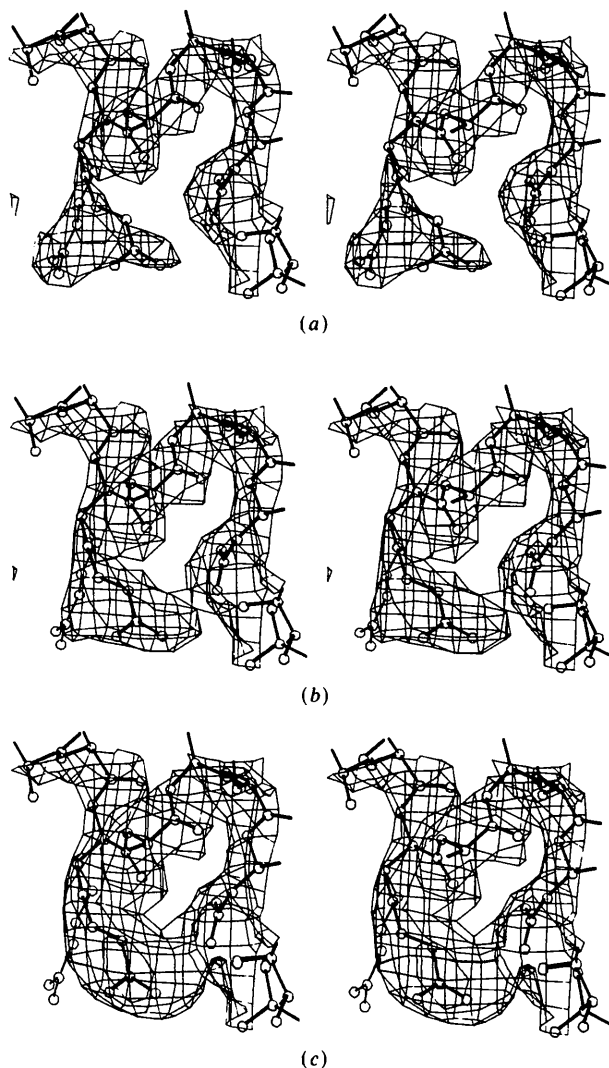
Fig. 5. Hybrid difference maps calculated from simulated TMV data, with the side chain of Arg 112 perturbed. Bessel order separations were taken from the complete perturbed structure, and phases of G terms from the partial structure, omitting residues 111–120. Coefficients used were (in the convention defined in the text): (a) $[2\mathcal{G} - \mathcal{G}_{omit}]$; (b) $[2(2\mathcal{G} - \mathcal{G}_0) - \mathcal{G}_{omit}]$; (c) $[2(3\mathcal{G} - 2\mathcal{G}_{omit})]$. Heavy lines: the TMV model used as the 'true' structure. Light lines: the perturbed structure. The coefficients used in Fig. 5(c) are related to those of Fig. 3(f).

increasingly practical (Namba & Stubbs, 1985, 1987), as is refinement of such structures (Namba & Stubbs, 1986; Stubbs, Namba & Makowski, 1986). Calculation of difference maps provides a valuable extension to these methods, as well as a means of correction during the progress of a refinement. Such maps have almost always been a necessary part of the crystallographic refinement of protein structures. As part of the refinement strategy in determining the structure of TMV at 2·9 Å resolution, we have used the types of maps described here to determine the location of about 35 water molecules associated with the viral coat protein subunit, as well as to correct the conformations of a number of side chains. An example is given in Fig. 6.

Determination of one structure makes possible the rapid determination of related structures, and these methods are being applied to closely related strains of TMV, and to TMV under conditions where small conformational changes in the coat protein are expected. More distantly related structures can be solved with limited numbers of heavy-atom derivatives, at a considerable saving in time compared with complete multi-dimensional phase determination (Namba & Stubbs, 1987), and errors in such structures can easily be detected with difference methods. Such a strategy would be appropriate, for example, for cucumber green mottle mosaic virus (Lobert, Heil, Namba & Stubbs, 1986).

Fibrous assemblies are made up of smaller units, which in many cases may be crystallizable. Actin
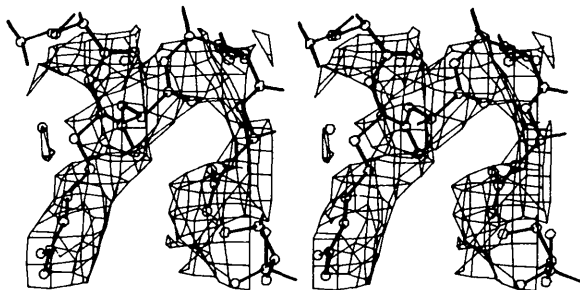
(Kabsch, Mannherz & Suck, 1985) and TMV coat protein (Bloomer, Champness, Bricogne, Staden & Klug, 1978) are only two of numerous possible examples. In such cases, a conformational change in the macromolecule is required in order to change the form of the assembly, but if the crystal structure can be determined it could provide a starting model for the determination of the fiber structure. An approach combining crystallography, fiber diffraction with limited numbers of heavy-atom derivatives, refinement of atomic coordinates and difference Fourier–Bessel syntheses is likely to play an important part in fiber diffraction studies of macromolecules in the future.

Fig. 6. A difference map of TMV using real data at 2·9 Å resolution, with coefficients $6\mathscr{F} - 5\mathscr{F}_0$. The side chain of Arg 112 was omitted from the model data, in order to check its conformation. It returns clearly in the electron density map, with perhaps a small adjustment indicated. (The side chain here is different from that of the other figures; in those cases, which used simulated data, the perturbed structure was used as the 'true' structure.) Maps such as these have been used extensively as part of the refinement of the TMV structure. We thank Dr Rekha Pattanayek for this example.

References

ARTYMIUK, P. J. & BLAKE, C. C. F. (1981). *J. Mol. Biol.* **152**, 737–762.

BLOOMER, A. C., CHAMPNESS, J. N., BRICOGNE, G., STADEN, R. & KLUG, A. (1978). *Nature (London)*, **276**, 362–368.

BLOW, D. M. & CRICK, F. H. C. (1959). *Acta Cryst.* **12**, 794–802.

BLUNDELL, T. L. & JOHNSON, L. N. (1976). *Protein Crystallography.* New York: Academic Press.

DEISENHOFER, J. & STEIGEMANN, W. (1975). *Acta Cryst.* B**31**, 238–250.

FRANKLIN, R. E. & KLUG, A. (1955). *Acta Cryst.* **8**, 777–780.

FUREY, W. F., ROBBINS, A. H., CLANCY, L. L., WINGE, D. R., WANG, B. C. & STOUT, C. D. (1986). *Science*, **231**, 704–710.

GLUSKER, J. P. & TRUEBLOOD, K. N. (1985). *Crystal Structure Analysis.* Oxford Univ. Press.

HENDERSON, R. & MOFFAT, J. K. (1971). *Acta Cryst.* B**27**, 1414–1420.

JONES, T. A. (1982). In *Computational Crystallography*, edited by D. SAYRE, pp. 303–317. Oxford Univ. Press.

KABSCH, W., MANNHERZ, H. G. & SUCK, D. (1985). *EMBO J.* **4**, 2113–2118.

KLUG, A., CRICK, F. H. C. & WYCKOFF, H. W. (1958). *Acta Cryst.* **11**, 199–213.

LOBERT, S., HEIL, P. D., NAMBA, K. & STUBBS, G. (1986). *Biophys. J.* **49**, 528a.

LUZZATI, V. (1953). *Acta Cryst.* **6**, 142–152.

MANDELKOW, E., STUBBS, G. & WARREN, S. (1981). *J. Mol. Biol.* **152**, 375–386.

NAMBA, K. & STUBBS, G. (1985). *Acta Cryst.* A**41**, 252–262.

NAMBA, K. & STUBBS, G. (1986). *Science*, **231**, 1401–1406.

NAMBA, K. & STUBBS, G. (1987). *Acta Cryst.* A**43**, 64–69.

SIM, G. A. (1959). *Acta Cryst.* **12**, 813–815.

STUBBS, G. & DIAMOND, R. (1975). *Acta Cryst.* A**31**, 709–718.

STUBBS, G. & MAKOWSKI, L. (1982). *Acta Cryst.* A**38**, 417–425.

STUBBS, G., NAMBA, K. & MAKOWSKI, L. (1986). *Biophys. J.* **49**, 58–60.

WASER, J. (1955). *Acta Cryst.* **8**, 142–150.